0022-3565/08/3243-1064–1072$20.00
THE JOURNAL OF PHARMACOLOGY AND EXPERIMENTAL THERAPEUTICS
JPET 324:1064–1072, 2008

Vol. 324, No. 3
131318/3312713
Printed in U.S.A.

Identification and Design of Peptides as a New Drug Delivery System for the Brain

Michel Demeule, Anthony Régina, Christian Ché, Julie Poirier, Tran Nguyen, Reinhard Gabathuler, Jean-Paul Castaigne, and Richard Béliveau

Laboratoire de Médecine Moléculaire, Centre d'Hémato-Oncologie, Hôpital Ste-Justine-Université du Québec à Montréal, Montréal, Québec, Canada (A.R., J.P., R.B.); and Angiochem, Montreal, Quebec, Canada (M.D., C.C., T.N., R.G., J.-P.C.)

Received September 13, 2007; accepted December 20, 2007

ABSTRACT

By controlling access to the brain, the blood-brain barrier (BBB) restricts the entry of proteins and potential drugs to cerebral tissues. We demonstrate here the transcytosis ability of aprotinin and peptides derived from Kunitz domains using an in vitro model of the BBB and in situ brain perfusion. Aprotinin transcytosis across bovine brain capillary endothelial cell (BBCEC) monolayers is at least 10-fold greater than that of holo-transferrin. Sucrose permeability was unaffected by high concentrations of aprotinin, indicating that transcytosis of aprotinin was unrelated to changes in the BBCEC monolayer integrity. Alignment of the amino acid sequence of aprotinin with the Kunitz domains of human proteins allowed the identification and design of a family of peptides, named Angiopeps. These peptides, and in particular Angiopep-2, exhibit higher transcytosis capacity and parenchyma accumulation than aprotinin. Overall, these results suggest that these Kunitz-derived peptides could be advantageously used as a new brain delivery system for pharmacological agents that do not readily enter the brain.

Blood-brain barrier (BBB) permeability is frequently a rate-limiting factor for the penetration of proteins, pharmacological agents, or peptides into the central nervous system (CNS) (Pardridge, 1999; Bickel et al., 2001). The BBB is mainly formed by brain capillary endothelial cells that are closely sealed by tight junctions. Brain capillaries also possess few fenestrae and few endocytic vesicles, compared with the capillaries of other organs (Pardridge, 1999). There is little transit across the BBB of large, hydrophilic molecules aside from some specific proteins such as transferrin, lactoferrin, and low-density lipoproteins, which are taken up by receptor-mediated endocytosis (Fillebeen et al., 1999; Pardridge, 1999; Tsuji and Tamai, 1999). It has been estimated and reported that the transport of small molecules across the BBB is the exception rather than the rule and that 98% of all small molecules do not cross the BBB (Pardridge, 2005). Because most drugs do not cross the BBB, few treatments are available against most CNS disorders, including Parkinson's disease, Alzheimer's disease, and brain cancers (Pardridge, 2001, 2005). Several approaches have been described for drug delivery to the brain, such as local invasive delivery by direct injection or infusion, induction of enhanced permeability, and various physiological targeting strategies (Begley, 2004; Gaillard et al., 2005; Pardridge, 2006).

Different transporters and receptors present at the BBB have been described as playing roles in maintaining the integrity of the BBB and brain homeostasis. Among them, the low-density lipoprotein receptor-related protein (LRP) has been reported to possess the ability to mediate transport of ligands across endothelial cells of the BBB (Shibata et al., 2000; Ito et al., 2006; Bell et al., 2007). For example, the passage of two members of the transferrin family, lactoferrin and melanotransferrin, involves LRP (Fillebeen et al., 1999; Demeule et al., 2002). It has also been proposed that the receptor-associated protein (RAP) can be efficiently transferred from the blood to the brain by LRP-mediated transcytosis (Pan et al., 2004). LRP has also been suggested to mediate the brain uptake of the tissue type plasminogen activator (Benchenane et al., 2005). Both LRP and megalin (LRP2) have been shown to be responsible for the endocytosis of secreted β-amyloid precursor protein (APP) (Kounnas et al., 1995; Cam and Bu, 2006). Interestingly, it has been

This work was supported by research funding from the National Research Council Canada Industrial Research Assistance Program to Angiochem and by a grant from National Sciences and Engineering Research Council of Canada (to R.B.).

Article, publication date, and citation information can be found at http://jpet.aspetjournals.org.

doi:10.1124/jpet.107.131318.

ABBREVIATIONS: BBB, blood-brain barrier; CNS, central nervous system; LRP, low-density lipoprotein receptor-related protein; RAP, receptor-associated protein; APP, amyloid precursor protein; KPI, Kunitz protease inhibitor; BBCEC, bovine brain capillary endothelial cell; BSA, bovine serum albumin; PBS, phosphate-buffered saline; HPLC, high-performance liquid chromatography; TCA, trichloroacetic acid; LDL, low-density lipoprotein; V_d, volume of distribution.

demonstrated that APP lacking the Kunitz protease inhibitor (KPI) domain is a poor substrate for LRP, suggesting that this domain is important for the recognition, internalization, and clearance of APP by LRP (Kounnas et al., 1995).

Aprotinin, a 6500-Da protease inhibitor is a LRP and LRP2 ligand, and also possesses a KPI domain (Moestrup et al., 1995; Hussain et al., 1999). In the present study, we investigated whether aprotinin crosses the BBB. To verify this hypothesis, we evaluated the transcytosis of aprotinin using both a well established in vitro model of the BBB (Dehouck et al., 1992; Fillebeen et al., 1999) and in situ brain perfusion in mice (Dagenais et al., 2000). The in vitro model consists of a coculture of bovine brain capillary endothelial cells (BBCEC) and rat glial cells. It presents ultrastructural features characteristic of brain endothelium, including tight junctions, lack of fenestration, lack of transendothelial channels, low permeability for hydrophilic molecules, and a high electrical resistance (Dehouck et al., 1992). The results obtained with in vitro and in vivo models provided evidence for greater passage of aprotinin across the BBB than of holo-transferrin. We identified a family of peptides, named Angiopeps, that were derived from the Kunitz domain and that demonstrated higher transcytosis capacity than did aprotinin. Overall, these are the first results indicating that Angiopeps could be used as a peptide-based delivery technology that provides a noninvasive and flexible platform for transporting drugs or biologically active molecules into the central nervous system.

Materials and Methods

Materials

Aprotinin, bovine serum albumin (BSA), lactoferrin, holo-transferrin, human antibodies (IgG), and iodo-beads were purchased from Sigma-Aldrich (Oakville, ON, Canada) whereas RAP was from Oxford Biomedical Research (Oxford, MI). Peptides (Angiopep-1, -2, -5, and -7) were synthesized by Peptidec (Pierrefonds, QC, Canada), whereas the 96 peptides were from Synpep (Dublin, CA). Angiopep-2 was also synthesized by Peptisyntha (Torrance, CA). Bovine brain endothelial cells, rat astrocytes, and serum for the in vitro BBB models were purchased from Cellial Technologies (Lens, France). Other biochemical reagents were purchased from Sigma-Aldrich.

Iodination of Proteins

Proteins (aprotinin, transferrin, human IgG, RAP, and BSA) and peptides were radiolabeled with standard procedures using an iodo-beads kit and D-Salt dextran desalting columns from Pierce Chemical (Rockford, IL). A ratio of two iodo-beads per aprotinin was used for the labeling. In brief, beads were washed twice with 3 ml of PBS on a Whatman filter and resuspended in 60 μl of PBS. $Na^{125}I$ (1 mCi) from GE Healthcare (Baie d'Urfé, QC, Canada) was added to the bead suspension for 5 min at room temperature. Iodination of each protein was initiated by the addition of 100 μg of protein (80–100 μl) diluted in 0.1 M phosphate buffer solution, pH 6.5. After incubation for 10 min at room temperature, iodo-beads were removed, and the supernatants were applied onto a desalting column prepacked with 5 ml of cross-linked dextran from Pierce Chemical. ^{125}I-proteins were eluted with 10 ml of PBS (150 mM NaCl, 2.7 mM KCl, 1.3 mM KH_2PO_4, and 8.1 mM $Na_2HPO_4{\cdot}7H_2O$). Fractions of 0.5 ml were collected, and the radioactivity in 5 μl from each fraction was measured. Fractions corresponding to ^{125}I-proteins were pooled and dialyzed (10–12-kDa cut-off) against Ringer/HEPES (150 mM NaCl, 5.2 mM KCl, 2.2. mM $CaCl_2$, 0.2 mM $MgCl_2{\cdot}6H_2O$), 6 mM $NaHCO_3$, 5 mM HEPES, and 2.8 mM glucose, pH 7.4). Kunitz-derived peptides were radioiodinated using the same procedures as for aprotinin. After the screening of the peptides, Angiopeps-1, -2, -5, and -7 were radiolabeled using iodo-beads and the same procedures. ^{125}I-Angiopeps were purified by hydrophobic chromatography using 30 RPC resin (GE Healthcare) to remove free iodine. Purified radiolabeled peptides were then analyzed by HPLC and C18 column.

In Vitro Transcytosis Studies

Preparation of Astrocytes. Primary cultures of mixed astrocytes were prepared from cerebral cortices of newborn rats (Dehouck et al., 1992). In brief, after removing the meninges, the brain tissue was gently forced through an 82-μm nylon sieve. Astrocytes were plated on six-well microplates at a concentration of 1.2×10^5 cells/ml in 2 ml of optimal culture medium (Dulbecco's modified Eagle's medium) supplemented with 10% heat-inactivated fetal calf serum, 2 mM glutamine, and 50 μg/ml gentamycin, The medium was changed twice a week. BBCECs were cultured in the presence of Dulbecco's modified Eagle's medium supplemented with heat-inactivated 10% (v/v) horse and 10% calf sera, 2 mM glutamine, 50 μg/ml gentamycin, and 1 ng/ml basic fibroblast growth factor, added every other day.

Blood-Brain Barrier Model. The in vitro model of BBB was established by using a coculture of BBCECs obtained from Cellial Technologies and newborn rat astrocytes as described previously (Dehouck et al., 1992). In brief, before cell coculture, plate inserts (Millicell-PC 3.0 μM, 30 mm in diameter; Millipore Corporation, Billerica, MA) were coated on the upper surface with rat tail collagen. They were then set in the six-multiwell microplates containing astrocytes prepared as described above, and BBCECs were plated on the upper side of the filters in 2 ml of coculture medium. BBCEC medium was changed three times a week. Under these conditions, differentiated BBCECs formed a confluent monolayer after 7 days. Experiments were performed between 5 and 7 days after confluence was reached. The number of cells at confluence was 400,000 cells/4.2 cm^2 or 90 μg of protein/4.2 cm^2, as evaluated by a micro-bicinchoninic acid assay from Pierce Chemical. For the screening of the 96 peptides, 1.1-cm^2 filters were used.

Transcytosis Experiments. Transcytosis experiments were performed as follows. Filters were washed with Ringer/HEPES solution, and ^{125}I-protein or ^{125}I-peptide (10–250 nM) was then added to the solution bathing the upper side of the insert. Transcytosis of various ^{125}I-proteins were tested (aprotinin, RAP, transferrin, human IgG, and BSA) using this in vitro BBB model. At various times, the insert was sequentially transferred into a fresh well to avoid possible reendocytosis of proteins, peptides or Angiopep conjugates by the abluminal side of the BBCECs. At the end of the experiment, ^{125}I-proteins were quantified in 500 μl of the lower chamber of each well by precipitating them with TCA. TCA precipitation was performed by adding 250 μl of BSA 0.5% in Ringer/HEPES solution to the collected 500 μl followed by 500 μl of TCA 50% for a final concentration of 20%. After 10 min at 4°C, the tubes were centrifuged for 10 min at 10,000 rpm. Radioactivity in the pellet was estimated with a gamma scintillator counter. We also measured peptides in 50 μl of the lower chamber of each well by SDS-polyacrylamide gel electrophoresis. Peptides were separated on 12.5% Tricine gels, stained with Coomassie Blue.

Sucrose Permeability. The permeability coefficient for sucrose was measured to verify the integrity and tightness of the BBCEC monolayers. Brain endothelial cell monolayers grown on inserts were transferred to six-well plates containing 2 ml of Ringer/HEPES per well (basolateral compartment). In each apical chamber, the culture medium was replaced by Ringer/HEPES containing 74 nM [^{14}C]sucrose (PerkinElmer Life and Analytical Sciences, Boston, MA). At predetermined times, the inserts were removed into other wells. At the end of the experiment, the amounts of radiotracer in basolateral compartments were measured in a liquid scintillation counter. The permeability coefficient (Pe) for sucrose was calculated as described previously by Dehouck et al. (1992), using filters either coated with endothelial cells or uncoated. The results were plotted as the clearance of [^{14}C]sucrose (microliters) as a function of time (minutes). The permeability coefficient (Pe) was calculated as $1/Pe = (1/PSt -$

1/PSf)/filter area (4.2 cm^2), where PSt is the permeability × surface area of a filter of the coculture, and PSf is the permeability of a filter coated with collagen and astrocytes plated on the bottom side of the filter.

In Situ Mouse Brain Perfusion

Transport Studies. The initial uptake of ^{125}I-aprotinin, ^{125}I-peptides, or [^{14}C]inulin was measured using the in situ brain perfusion method adapted in our laboratory for the study of drug uptake in the mouse brain (Dagenais et al., 2000; Cisternino et al., 2001). In brief, the right common carotid artery of ketamine/xylazine (140/8 mg/kg i.p.)-anesthetized mice was exposed and ligated at the level of the bifurcation of the common carotid, rostral to the occipital artery. The common carotid was then catheterized rostrally with polyethylene tubing filled with 25 U/ml heparin, and it was mounted on a 26-gauge needle. The syringe containing the perfusion fluid (^{125}I-proteins in Krebs/bicarbonate buffer at pH 7.4, gassed with 95% O_2 and 5% CO_2) was placed in an infusion pump (pump PHD 2000; Harvard Apparatus Inc., Holliston, MA) and connected to the catheter. Before the perfusion, the contralateral blood flow contribution was eliminated by severing the heart ventricles. The brain was perfused for the indicated times (2.5–15 min) at a perfusion rate of 1.15 ml/min. After perfusion of radiolabeled molecules, the brain was further perfused for 60 s with Krebs buffer, to wash away excess ^{125}I-proteins. Mice were then decapitated to terminate perfusion, and the right hemisphere was isolated on ice before being subjected to capillary depletion. In brief, for capillary depletion, the mice brain was homogenized on ice in Ringer-HEPES buffer with 0.1% BSA in a glass homogenizer. Brain homogenate was then mixed thoroughly with 35% dextran 70 (50/50), and it was centrifuged at 5400*g* for 10 min at 4°C. The supernatant composed of brain parenchyma and the pellet representing capillaries were then carefully separated. Aliquots of homogenates, supernatants, pellets, and perfusates were taken to measure their contents of ^{125}I-proteins by TCA precipitation and to evaluate the apparent volume of distribution (V_d).

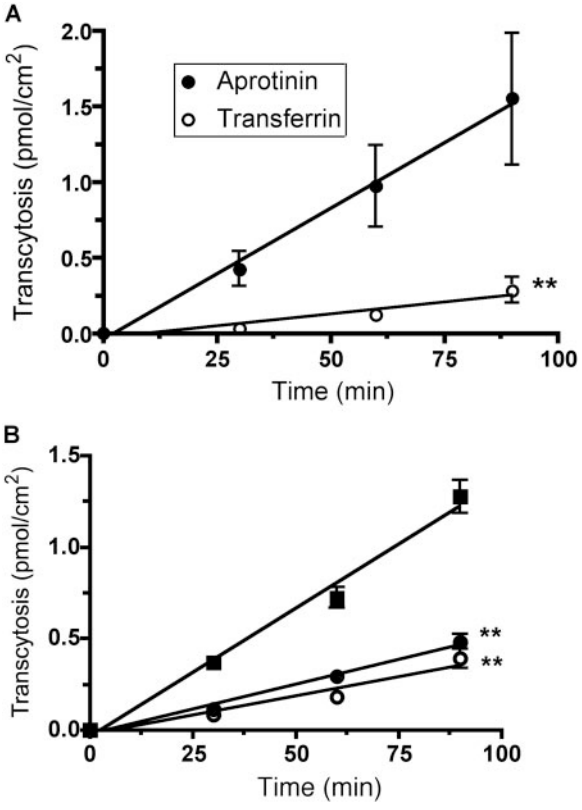

Fig. 1. Transport of ^{125}I-aprotinin through endothelial cell monolayers. A, transport of ^{125}I-aprotinin and ^{125}I-transferrin (50 nM) from the apical to the basolateral side of the in vitro BBB model was measured for 90 min. B, transcytosis of ^{125}I-aprotinin was measured at 37°C (black squares) and at 4°C (black circles). The transport experiment was also performed with denatured ^{125}I-aprotinin by heating it at 95°C for 5 min (open circles). Data represent the means ± S.D. **, $p < 0.01$, significant difference in the curve slope compared with aprotinin curve.

TABLE 1

Transcytosis of ^{125}I-proteins (250 nM) across BBCEC monolayers was measured for 1 h

Data represent the means ± S.D. obtained from at least three different filters for each protein. Numbers of filters are indicated in parentheses.

Protein	Transcytosis	Ratio (Aprotinin/Protein)
	$pmol/cm^2/h$	
Aprotinin	0.83 ± 0.2	1 (n = 11)
Transferrin	0.08 ± 0.02	10 (n = 6)
Nonspecific IgGs	0.05 ± 0.03	17 (n = 3)
RAP	0.06 ± 0.02	14 (n = 3)
BSA	0.05 ± 0.02	17 (n = 3)

Data Analysis

Data are expressed as mean ± S.D. Statistical analyses were performed using Student's t test when one group was compared with the control group. To compare two or more groups with the control group, one-way analysis of variance with Dunnett's post hoc test was used. In addition, curve slopes were used to determine whether two curves were statistically different. All statistical analyses were performed using GraphPad Prism version 4.0C for Macintosh (GraphPad Software Inc., San Diego, CA). Significance was assumed for p values less than 0.5.

Results

To evaluate and characterize the transcytosis of aprotinin, we used an in vitro model of the BBB. After iodination with Biobeads, transcytosis of 250 nM ^{125}I-aprotinin and ^{125}I-holo-transferrin across endothelial cells monolayers was compared using this model (Fig. 1). Transport from the apical to the basolateral side of ^{125}I-aprotinin was much higher than for ^{125}I-holo-transferrin. In addition, the effect of aprotinin on the BBB integrity was determined by measuring sucrose permeability in the presence or absence of a high aprotinin concentration (5 μM). The clearance of sucrose measured in the presence of aprotinin was similar to that measured for the control. Under both conditions, the sucrose permeability coefficient was equivalent, $0.45 \pm 0.05 \times 10^{-3}$ cm/min, indicating that aprotinin does not affect BBB integrity.

The passage of ^{125}I-aprotinin across BBCEC was also evaluated at 4°C (Fig. 1B). Aprotinin was boiled for 15 min to evaluate the transport rate of denatured-^{125}I-aprotinin. The transport rate of ^{125}I-aprotinin at 4°C was strongly reduced compared with that measured at 37°C. The passage of denatured-^{125}I-aprotinin was very similar to the transport value obtained at 4°C. These results indicate that transcytosis of ^{125}I-aprotinin from the apical to the basolateral side in this BBB model is sensitive to temperature and to the native conformation of aprotinin, suggesting that the transcytosis of ^{125}I-aprotinin involves a receptor.

The transport across the BBCEC monolayers of ^{125}I-aprotinin and other proteins at the same concentration (250 nM) is compared in Table 1. Transport rates are expressed in term of picomoles per squared centimeter per hour. These results indicate that ^{125}I-aprotinin transport is higher than

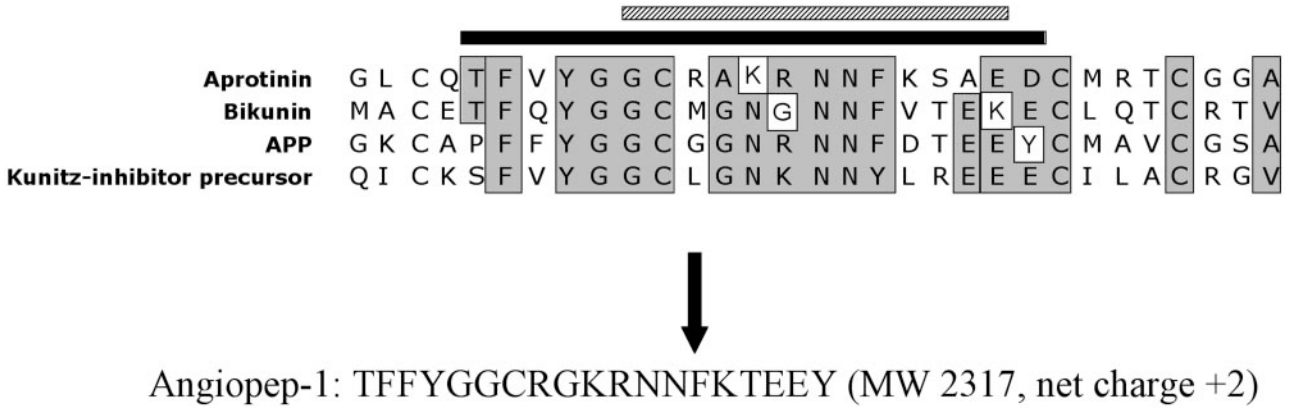

Fig. 2. Alignment of aprotinin with related proteins. The amino acid sequence of aprotinin was compared with a databank of protein sequences. The amino acid sequences of the proteins with the highest sequence similarity (bikunin, amyloid β A4 protein precursor, and the Kunitz inhibitor-1 precursor) were aligned with that of aprotinin. The hatched bar represents the minimal identified sequence for aprotinin interaction with LRP2 (Moestrup et al., 1995). From the sequences indicated in the black bar, 96 peptides were designed.

other proteins, including ^{125}I-transferrin, ^{125}I-lactoferrin, ^{125}I-streptavidin, ^{125}I-human IgGs, and ^{125}I-BSA. The ratios between the transendothelial transport rates of ^{125}I-aprotinin and these proteins indicate that the passage of aprotinin is at least 10-fold higher.

To identify the portion of aprotinin responsible for its transport, amino acid sequence homology was searched using protein BLAST program on the National Center for Biotechnology Information website (http://www.ncbi.nlm.nih.gov/). The search for the homology of C-terminal amino acid sequence of aprotinin (GLCQTFVYGGCRAKRNNFKSAE) resulted in 27 sequences being identified, some of which were human proteins. The proteins with the highest scores were then aligned with the sequence of aprotinin (Fig. 2). These proteins identified as APP, bikunin and KPI have a common property because they are LRP ligands (Herz and Strickland, 2001; Hussain et al., 1999). From this alignment, 96 peptides were designed and tested using the BBB in vitro model and in situ brain perfusion. The first level of screening was performed by SDS-polyacrylamide gel electrophoresis analysis (data not shown). In this approach, each peptide (1 mg/ml) was added to the apical side of endothelial cell monolayers. After 1 h, 50 μl of solution from the basolateral side of the monolayers was separated by electrophoresis. Gels were stained by Coomassie Blue and analyzed by densitometry. Peptides that were detected at the highest levels in the bottom chamber were radioiodinated, and then they were re-evaluated using the in vitro BBB model for the second level of screening (Table 2). Transcytosis of these peptides is expressed in terms of percentage of peptides recovered at the basolateral side compared with that initially added to the apical side of endothelial cell monolayers. In situ brain perfusion was then performed as a third level of screening (Table 3). Mice were perfused with ^{125}I-peptides for 5 min followed capillary depletion to assess their brain volume of distribution. The results in Table 3 show the volume of distribution in total brain, brain capillaries, and brain parenchyma of ^{125}I-peptides and the ratio between the distribution volumes measured for the parenchyma and total brain. A family of peptides was selected based on their parenchymal distribution volume. Peptides 5 and 8, which were positively charged (net charge +6), were mainly found associated with brain capillaries. Peptide 67 (called Angiopep-1) was selected, based on its high level of transcytosis and its brain parenchymal distribution volume.

Angiopep-1 was subsequently further modified for evaluation (Fig. 3A). First, the cysteine at position 7 was replaced by a serine to prevent peptide dimerization or the formation of disulfide bonds with serum proteins. The parenchymal

TABLE 2

Transcytosis of ^{125}I-peptides across BBCEC monolayers was measured for 1 h

Peptides were added to the apical side of BBCEC. After 1 h, the amount of ^{125}I-peptides in the lower compartment was quantified. The amount in the lower compartment was compared with that added to the apical side (initial value) and expressed as the percentage of transcytosis. Data represent the means ± S.D. obtained from at least three different filters for each peptide.

Peptide	Amino Acid Sequence	Transcytosis
		%
5	TFFYGGCRAKRNNFKRAKY	5.1 ± 0.8
8	TFFYGGCRGKKNNFKRAKY	3.9 ± 0.3
67[a]	TFFYGGCRGKRNNFKTEEY	15.8 ± 5.1
75	PFFYGGCRGKRNNFKTEEY	8.7 ± 0.7
76	TFFYGGCRGKRNNFKTKEY	8.4 ± 2.7
77	TFFYGGKRGKRNNFKTKEY	6.3 ± 2.3
78	TFFYGGCRGKRNNFKTKRY	7.5 ± 1.0
79	TFFYGGKRGKRNNFKTAEY	7.8 ± 0.7
81	TFFYGGKRGKRNNFKREKY	8.8 ± 0.4
90	RFKYGGCLGNKNNFLRLKY	13.4 ± 1.2
91	RFKYGGCLGNKNNYLRLKY	15.8 ± 3.3

[a] Also known as Angiopep-1.

TABLE 3

Volume of distribution for peptides

Brain perfusion was performed for 5 min with ^{125}I-peptides as described under *Materials and Methods*. Data correspond to means obtained after the perfusion of two mice. Data represent the means ± S.D. The ratios between the distribution volumes measured in parenchyma (P) and total brain (B) are also presented.

Peptide	Volume of Distribution			Ratio (P/B)
	Total B	Capillaries	P	
	ml/100 g/5 min			
5	312 ± 82	217 ± 25	95 ± 58	0.30
8	250 ± 26	204 ± 1	46 ± 26	0.18
67[a]	38 ± 1	13 ± 7.5	25 ± 8	0.66
76	40 ± 1.7	16 ± 5	24 ± 7	0.60
78	198 ± 84	181 ± 83	16 ± 1	0.08
79	70 ± 6	52 ± 11	18 ± 5	0.26
90	87 ± 41	76 ± 35	11 ± 7	0.13
91	47 ± 24	24 ± 7	23 ± 16	0.49

[a] Also known as Angiopep-1.

A

Peptides	Amino acid sequence	Net charge
Angiopep-1	TFFYGGCRGKRNNFKTEEY	+2
Angiopep-2	TFFYGG**S***RGKRNNFKTEEY	+2
Angiopep-5	TFFYGG**S***RGKRNNF**R***TEEY	+2
Angiopep-7	TFFYGG**S***RG**R***RNNF**R***TEEY	+2

B

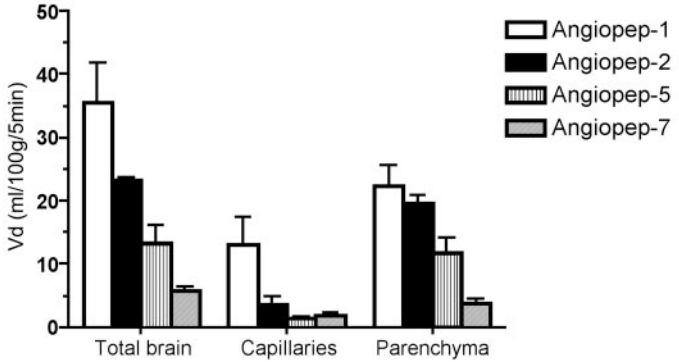

Fig. 3. Volumes of distribution of Angiopeps in the brain parenchyma measured by in situ brain perfusion. A, amino acid sequence of tested Angiopeps are presented. Changes in the amino acid sequence (when compared with Angiopep-1) are indicated in bold and with an asterisk. B, mice were perfused with 100 nM ^{125}I-Angiopeps for 5 min as described under *Materials and Methods*. After perfusion, brain capillary depletion was performed on the mice right brain hemispheres. The amount of radioactivity associated with total brain homogenate, the brain capillary fraction and the parenchyma was evaluated in a gamma counter. The results were expressed as the apparent V_d for the ^{125}I-Angiopeps found in these brain compartments. Data represent the means ± S.D. obtained for at least three mice.

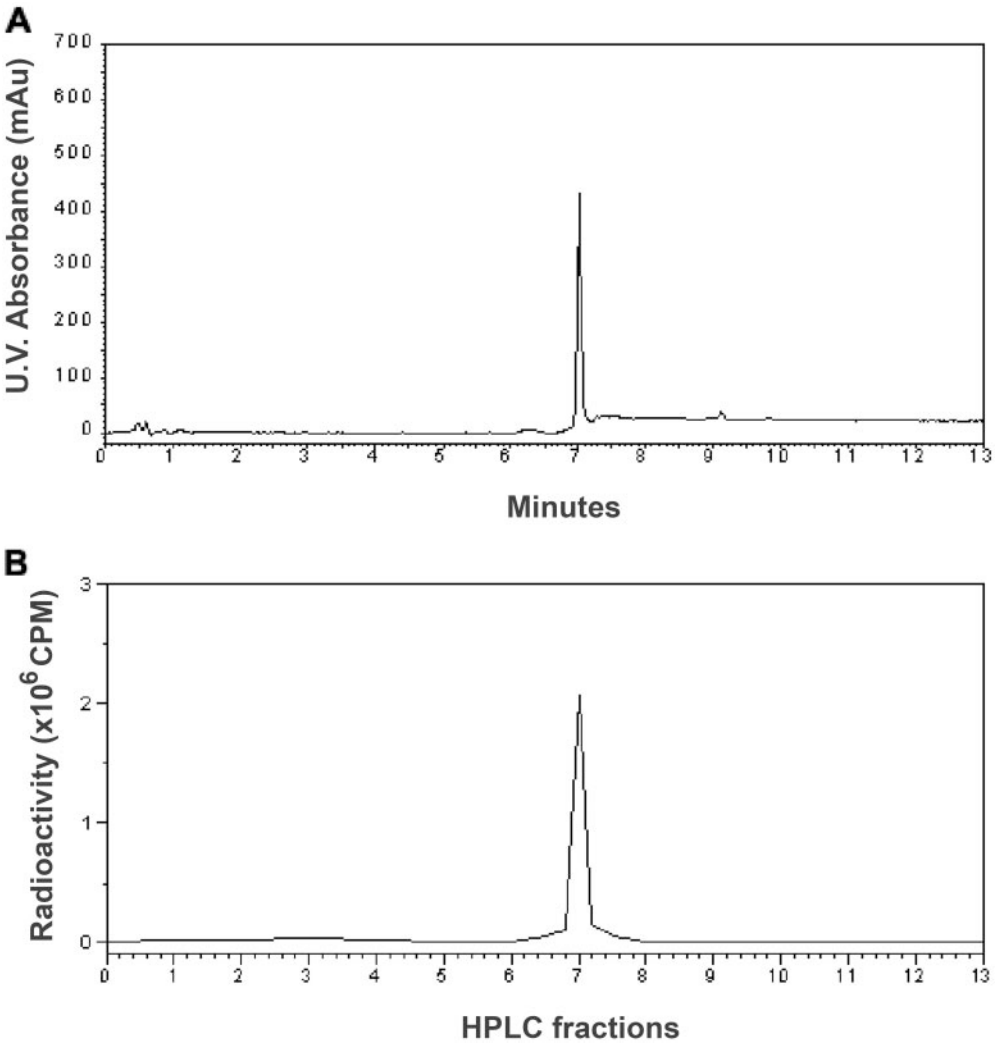

Fig. 4. HPLC analysis of ^{125}I-Angiopep-2. After the radiolabeling and purification of the labeled peptide on 30 RPC resin using AKTA explorer, HPLC analysis was performed at a flow rate of 1 ml/min to evaluate the incorporation of ^{125}I on Angiopep-2. A, the peptide was followed at a wavelength of 229 nm. B, fractions of 1 ml were collected, and the radioactivity associated with these fractions was quantified in a gamma counter. The major peak of radioactivity was found in the fraction 7, which corresponds to the retention time of the ^{125}I-Angiopep-2 (7 min).

uptake of this peptide (Angiopep-2), as measured by in situ brain perfusion, was similar to that of Angiopep-1 (Fig. 3B). Second, the lysine residue at position 10 was replaced by an arginine (creating Angiopep-5), whereas in Angiopep-7, the lysine at positions 10 and 15 were replaced by arginine residues. Each of these three peptides (Angiopep-2, Angiopep-5, and Angiopep-7) has a net charge of +2. However, parenchymal uptake for both Angiopep-5 and Angiopep-7 was decreased by approximately 60 and 85%, respectively. These results suggest that the replacement of the cysteine by a serine has a low impact on the parenchymal transport. In contrast, replacement of the lysine residues at positions 10 and 15 prevents the transport capacity.

An example of peptide radiolabeling is shown in Fig. 4. After the screening of the 96 peptides, the selected peptides were purified following iodination by reverse phase using 30RPC resin and AKTA explorer system to remove excess of free [^{125}I]iodine. Then, radiolabeled peptides were analyzed by HPLC on a C18 column at 229-nm wavelength. In Fig. 4A, a chromatogram of ^{125}I-Angiopep is presented. Fractions were collected and measured for radioactivity. As shown in Fig. 4B, the peak of radioactivity corresponds to the UV peak of Angiopep-2 detected in Fig. 4A. In this case, more than 92% of the radioactivity was found in this peak, and the specific activity estimated for ^{125}I-Angiopep-2 was 340,000 cpm/μg or 0.44 μCi/nmol.

We further characterized the transport of aprotinin and Angiopep-2 using the in vitro BBB model. As shown in Fig. 5A, Angiopep-2 transcytosis was also found to be 7-fold higher than that of aprotinin, confirming the results obtained by in situ brain perfusion. Transport from the apical to the basolateral side of ^{125}I-Angiopep-2 was much higher than for ^{125}I-aprotinin. Previous studies have showed that aprotinin is a ligand for receptor(s) of the LRP1 (α2-macroglobulin receptor) or LRP2 (megalin) (Moestrup et al., 1995). Here, to determine whether the transcytosis of aprotinin and Angio-

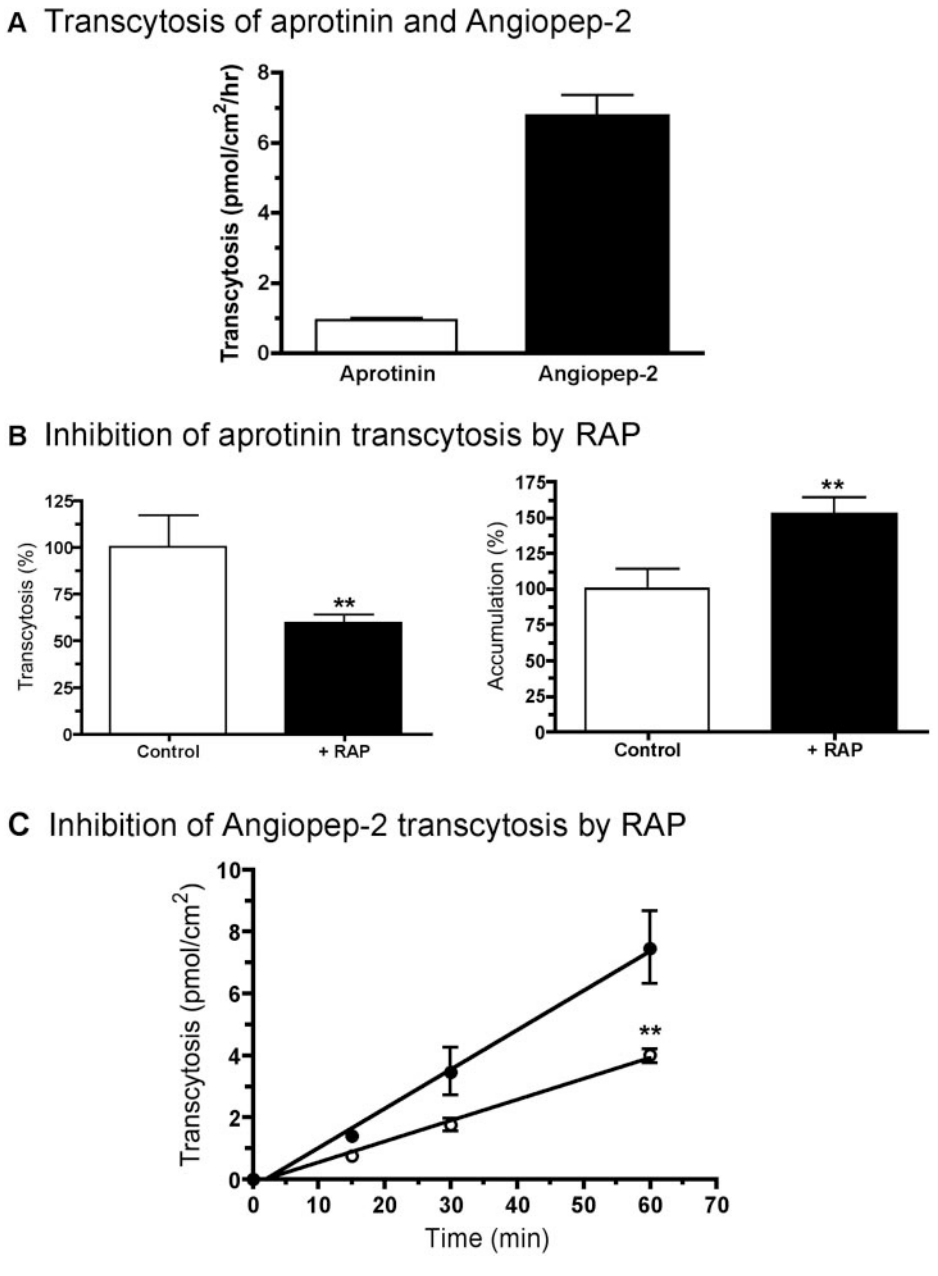

Fig. 5. Transcytosis of ^{125}I-Angiopep-2 from the apical to the basolateral side of endothelial cell monolayers. Transport of aprotinin and Angiopep-2 (250 nM) was measured from the apical to the basolateral side of the BBCEC monolayers as described under *Materials and Methods*.

pep-2 could involve LRP, we measured the impact of RAP, a chaperone protein for all members of the low-density lipoprotein (LDL)-receptor family, on the aprotinin transcytosis (Fig. 5B). The addition of RAP inhibited the transport of ^{125}I-aprotinin from the apical to the basolateral side of endothelial cell monolayers of this in vitro BBB model (Fig. 5B, left). By recuperating filters coated with BBCEC, we estimated the accumulation ^{125}I-aprotinin in these endothelial cells (Fig. 5B, right). In the presence of RAP, the inhibition of ^{125}I-aprotinin transcytosis also led to an increase in its accumulation in BBCECs. The transcytosis of Angiopep-2 was reduced by approximately 45% with the addition of RAP (Fig. 5C). Thus, the addition of RAP partially reduced the transcytosis of both aprotinin and Angiopep-2. This inhibition by RAP suggests that Angiopep-2 retains its capacity to interact with aprotinin receptor.

The apparent distribution volume of Angiopep-2 measured by in situ brain perfusion indicated that the brain and parenchymal volume of distribution for Angiopep-2 is much higher than for transferrin and aprotinin after 5 min perfusion (Fig. 6). Furthermore, the apparent distribution volume in brain parenchyma of Angiopep-2 increased linearly for at least 15 min of perfusion and was much higher than for the vascular marker [^{14}C]inulin (Fig. 7A). Moreover, the addition of Angiopep-2 (up to 500 nM) did not affect the volume of distribution for inulin (Fig. 7B), indicating that the BBB integrity was unaffected under these conditions by the peptide. To demonstrate that receptor-mediated transcytosis could participate in the transport of Angiopep-2 across the BBB, in situ brain perfusion was performed in the presence of an excess of unlabeled Angiopep-2. As shown in Fig. 8A, the addition of unlabeled Angiopep-2 (0.5 and 10 μM) to the perfusate reduced the brain V_d of ^{125}I-Angiopep-2 (0.025 μM) by 50%, whereas aprotinin at 10 μM reduced it by 40% (Fig. 8B). Overall, these data suggest that a portion of the transport of Angiopep-2 at the BBB is partially saturable and that receptor-mediated transcytosis is involved.

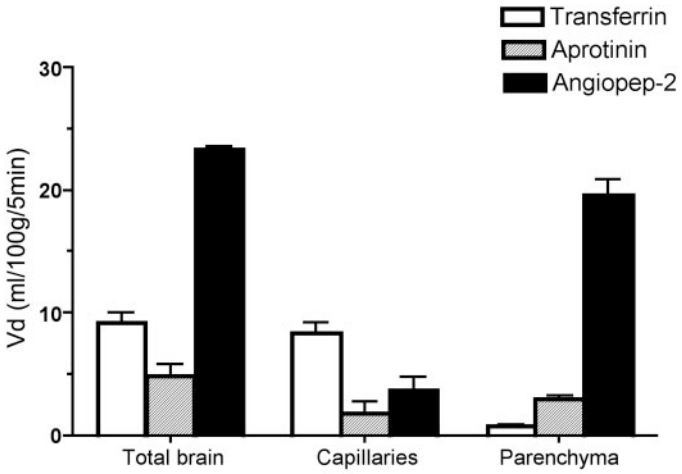

Fig. 6. Effect of RAP on aprotinin and Angiopep transcytosis across BBCEC monolayers. A, transcytosis (left) across BBCEC monolayers and accumulation inside BBCECs (right) of ^{125}I-aprotinin were measured for 1 h in the presence or absence of 50 μg/ml RAP as described under *Materials and Methods*. Data represent the means ± S.D. obtained from three different experiments performed in triplicate. B, transcytosis of ^{125}I-Angiopep-2 was also evaluated in the presence of RAP. Data represent the means ± S.D. obtained from six different filters. *, $p < 0.05$, significant difference compared with control.

Discussion

In the development of new therapies to treat brain pathologies, the BBB is a major obstacle against the use of potential drugs for treating disorders of the CNS (Begley, 2004). In the present study, we report that peptides derived from the Kunitz domain have a higher brain penetration capability than do other proteins, such as transferrin, as shown using both an in vitro model of the BBB and in situ brain perfusion in mice. These data suggest that Angiopep could be used as a brain delivery system for macromolecules.

We first demonstrated here that aprotinin transcytosis across BBCEC monolayers is at least 8-fold higher than that of transferrin. This high transcytosis of aprotinin was not related to changes in the BBCEC monolayer integrity as measured by the sucrose permeability. The temperature and conformation dependence of the transendothelial transport of aprotinin suggest the involvement of a mechanism implicating receptor-mediated transcytosis. Previous studies using technetium-99m-labeled aprotinin, which requires partial reduction of the protein disulfide bonds and the chelation of the generated sulfhydryl groups, have reported low brain accumulation compared with other tissues (kidney and liver) (Schaadt et al., 2003; Sojan et al., 2005). Here, transcytosis using both an in vitro BBB model and in situ brain perfusion clearly showed that aprotinin crosses the BBB much more efficiently than other proteins. The brain accumulation and the high rate of aprotinin transcytosis suggested that aprotinin or an aprotinin-derived peptide could be advantageously used as a new delivery system for the brain.

To identify the minimal sequence required for transport of aprotinin across the BBB, we looked for sequence homologies with other proteins having similar properties. Several hits were obtained with the C-terminal portion, which includes the Kunitz domain of aprotinin. Alignment of proteins with the highest scores allowed us to design more than 96 human aprotinin-derived peptides. These peptides were tested using the BBB in vitro model and in situ brain perfusion. From these results, a family of peptides derived from the Kunitz domain of human proteins was selected and called Angiopeps. These peptides have higher apparent brain volume of distribution than aprotinin. Among them, Angiopep-2 was selected and further characterized.

Other peptides have been proposed as a drug delivery system, such as the polybasic peptides SynB1, SynB4, and peptides derived from Antennapedia and PD-TAT proteins from human immunodeficiency virus (Drin et al., 2003; Dietz and Bahr, 2004; Peng et al., 2004). These peptides are highly positively charged, and absorptive-mediated transcytosis has been proposed for their transport across the BBB. A bradykinin analog [H-Arg-Pro-Hyp-Gly-Thi-Ser-Pro-4-Me-Tyr(psi CH2NH)-Arg-OH or Cereport] has also been reported to increase the penetration of small molecules such as carboplatin by transitory opening of the BBB (Borlongan and Emerich, 2003). The exact molecular mechanism of Angiopep transcytosis remains to be established. However, the fact that these peptides are derived from aprotinin and human proteins known to interact with the LDL receptor related protein family (LRP1 or LRP2, also known as megalin) and that they contain a fragment responsible for the interaction with these receptors suggest a receptor-mediated transport mechanism

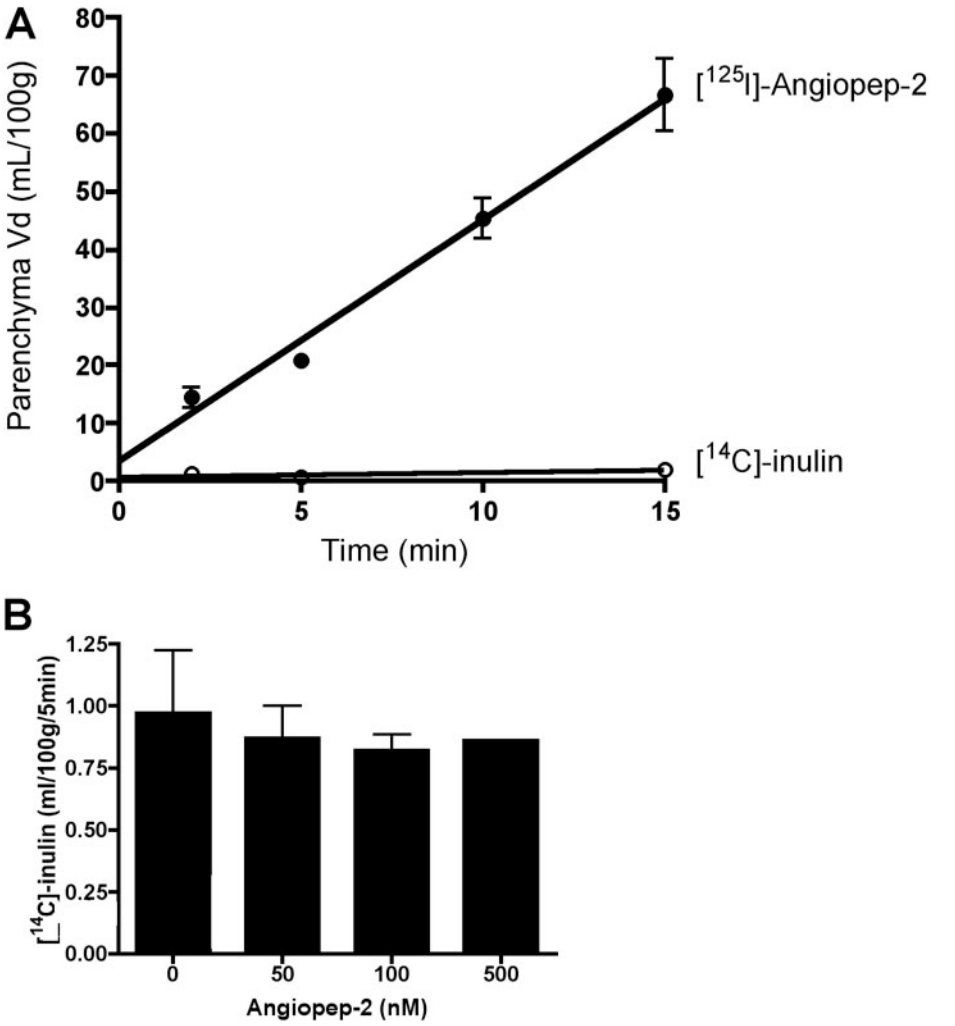

Fig. 7. Distribution volume of Angiopep-2 in mice brain parenchyma. A, apparent volume of distribution in the brain parenchyma was measured at different perfusion times for both ^{125}I-Angiopep-2 and the vascular marker [^{14}C]inulin. B, effect of Angiopep-2 concentration on the parenchyma apparent volume of [^{14}C]inulin was also measured for a 5-min perfusion.

for aprotinin and Angiopeps. The decrease by approximately 50% in the V_d of ^{125}I-Angiopep-2 in the presence of excess unlabeled Angiopep-2 (10 μM) suggests also that a part in the transport of this peptide is associated with a receptor. This is in agreement with the inhibition of ^{125}I-urokinase-plasminogen activator inhibitor-1 complex to LRP1 and LRP2 by aprotinin, which has been reported to be in the same range (4 μM) (Moestrup et al., 1995). In addition, partial inhibition of aprotinin and Angiopep-2 transcytosis by RAP, which was previously shown to inhibit the binding of all ligands to all members of the LDL-family receptor, also indicates that the passage of both molecules across brain endothelial cells involves LRP-mediated events.

These are the first results showing that peptides derived from human Kunitz domains could be used as a potential delivery system for macromolecules. To date, various attempts have been made to identify and characterize an efficient drug delivery approach for the brain (Demeule et al., 2004; de Boer and Gaillard, 2007; Pardridge, 2007a). Different strategies are now under investigation for peptide and protein drug delivery to the brain. Invasive procedures include the direct intraventricular administration of drugs by means of surgery, and the temporary disruption of the BBB via intracarotid infusion of hyperosmolar solutions (Doolittle et al., 2000; Hall et al., 2006). Pharmacologically based strategies include facilitating passage through the BBB by increasing the lipid solubility of peptides or proteins (Zhou et al., 2002). Physiologically based strategies exploiting the various carrier mechanisms at the BBB have been characterized in the recent years (Pardridge, 2006, 2007b). In this approach, drugs are attached to a protein vector that performs like a receptor-targeted delivery vehicle at the BBB. This approach is highly specific and presents high efficacy with extreme flexibility for clinical indications with unlimited targets. Overall, the results obtained in the present study with aprotinin and Angiopep suggest that their transcytosis involves a member of the LDL-receptor family. These receptors are known to share various ligands and protein complexes of high molecular weight (Hussain et al., 1999; May et al., 2007). Thus, our data suggest that these receptors could be advantageously used to transport small molecules, and high-molecular-weight peptides or proteins such as therapeutic monoclonal antibodies, across the BBB.

In conclusion, these are the first in vitro and in vivo results showing that aprotinin and aprotinin-derived peptides have a higher ability to accumulate in the brain than other proteins such as transferrin and RAP. Taken together, our results indicate that Kunitz-derived peptides could be advantageously used as a new brain delivery system. Further work is now underway with various therapeutic targets, including

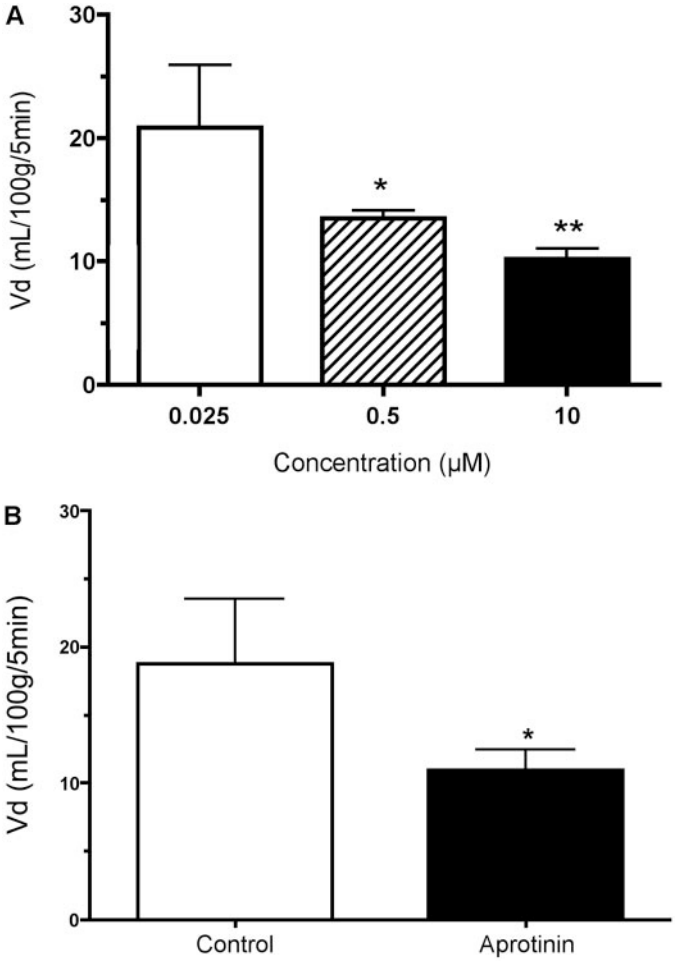

Fig. 8. Effect of excess Angiopep-2 on its brain V_d. A, V_d in the brain was measured for 0.025 μM ^{125}I-Angiopep with and without 0.5 and 10 μM unlabeled Angiopep-2. Data represent the means ± S.D. obtained from the perfusion of at least five mice. *, $p < 0.01$ and **, $p < 0.001$, significant difference compared with 0.025 μM ^{125}I-Angiopep-2 using one-way analysis of variance). B, V_d in the brain was also measured for 0.025 μM ^{125}I-Angiopep in the absence (control) or in the presence of 10 μM aprotinin. Data represent the means ± S.D. obtained from the perfusion of 10 mice for the control and three for aprotinin. *, $p < 0.02$.

small-molecule macromolecules or other pharmaceutical agents.

Acknowledgments

We thank Isabelle Lavallée and Marie-Paule Lachambre for technical support.

References

Begley DJ (2004) Delivery of therapeutic agents to the central nervous system: the problems and the possibilities. *Pharmacol Ther* **104:**29–45.
Bell RD, Sagare AP, Friedman AE, Bedi GS, Holtzman DM, Deane R, and Zlokovic BV (2007) Transport pathways for clearance of human Alzheimer's amyloid beta-peptide and apolipoproteins E and J in the mouse central nervous system. *J Cereb Blood Flow Metab* **27:**909–918.
Benchenane K, Berezowski V, Fernandez-Monreal M, Brillault J, Valable S, Dehouck MP, Cecchelli R, Vivien D, Touzani O, and Ali C (2005) Oxygen glucose deprivation switches the transport of tPA across the blood-brain barrier from an LRP-dependent to an increased LRP-independent process. *Stroke* **36:**1065–1070.
Bickel U, Yoshikawa T, and Pardridge WM (2001) Delivery of peptides and proteins through the blood-brain barrier. *Adv Drug Deliv Rev* **46:**247–279.
Borlongan CV and Emerich DF (2003) Facilitation of drug entry into the CNS via transient permeation of blood brain barrier: laboratory and preliminary clinical evidence from bradykinin receptor agonist, Cereport. *Brain Res Bull* **60:**297–306.
Cam JA and Bu G (2006) Modulation of beta-amyloid precursor protein trafficking and processing by the low density lipoprotein receptor family. *Mol Neurodegener* **1:**8.
Cisternino S, Rousselle C, Dagenais C, and Scherrmann JM (2001) Screening of multidrug-resistance sensitive drugs by in situ brain perfusion in P-glycoprotein-deficient mice. *Pharm Res* **18:**183–190.
Dagenais C, Rousselle C, Pollack GM, and Scherrmann JM (2000) Development of an in situ mouse brain perfusion model and its application to mdr1a P-glycoprotein-deficient mice. *J Cereb Blood Flow Metab* **20:**381–386.
de Boer AG and Gaillard PJ (2007) Drug targeting to the brain. *Annu Rev Pharmacol Toxicol* **47:**323–355.
Dehouck MP, Jolliet-Riant P, Bree F, Fruchart JC, Cecchelli R, and Tillement JP (1992) Drug transfer across the blood-brain barrier: correlation between in vitro and in vivo models. *J Neurochem* **58:**1790–1797.
Demeule M, Poirier J, Jodoin J, Bertrand Y, Desrosiers RR, Dagenais C, Nguyen T, Lanthier J, Gabathuler R, Kennard M, et al. (2002) High transcytosis of melanotransferrin (P97) across the blood-brain barrier. *J Neurochem* **83:**924–933.
Demeule M, Regina A, Annabi B, Bertrand Y, Bojanowski MW, and Beliveau R (2004) Brain endothelial cells as pharmacological targets in brain tumors. *Mol Neurobiol* **30:**157–183.
Dietz GP and Bahr M (2004) Delivery of bioactive molecules into the cell: the Trojan horse approach. *Mol Cell Neurosci* **27:**85–131.
Doolittle ND, Miner ME, Hall WA, Siegal T, Jerome E, Osztie E, McAllister LD, Bubalo JS, Kraemer DF, Fortin D, et al. (2000) Safety and efficacy of a multicenter study using intraarterial chemotherapy in conjunction with osmotic opening of the blood-brain barrier for the treatment of patients with malignant brain tumors. *Cancer* **88:**637–647.
Drin G, Cottin S, Blanc E, Rees AR, and Temsamani J (2003) Studies on the internalization mechanism of cationic cell-penetrating peptides. *J Biol Chem* **278:**31192–31201.
Fillebeen C, Descamps L, Dehouck MP, Fenart L, Benaissa M, Spik G, Cecchelli R, and Pierce A (1999) Receptor-mediated transcytosis of lactoferrin through the blood-brain barrier. *J Biol Chem* **274:**7011–7017.
Gaillard PJ, Visser CC, and de Boer AG (2005) Targeted delivery across the blood-brain barrier. *Expert Opin Drug Deliv* **2:**299–309.
Hall WA, Doolittle ND, Daman M, Bruns PK, Muldoon L, Fortin D, and Neuwelt EA (2006) Osmotic blood-brain barrier disruption chemotherapy for diffuse pontine gliomas. *J Neurooncol* **77:**279–284.
Herz J and Strickland DK (2001) LRP: a multifunctional scavenger and signaling receptor. *J Clin Invest* **108:**779–784.
Hussain MM, Strickland DK, and Bakillah A (1999) The mammalian low-density lipoprotein receptor family. *Annu Rev Nutr* **19:**141–172.
Ito S, Ohtsuki S, and Terasaki T (2006) Functional characterization of the brain-to-blood efflux clearance of human amyloid-beta peptide (1-40) across the rat blood-brain barrier. *Neurosci Res* **56:**246–252.
Kounnas MZ, Moir RD, Rebeck GW, Bush AI, Argraves WS, Tanzi RE, Hyman BT, and Strickland DK (1995) LDL receptor-related protein, a multifunctional ApoE receptor, binds secreted beta-amyloid precursor protein and mediates its degradation. *Cell* **82:**331–340.
May P, Woldt E, Matz RL, and Boucher P (2007) The LDL receptor-related protein (LRP) family: an old family of proteins with new physiological functions. *Ann Med* **39:**219–228.
Moestrup SK, Cui S, Vorum H, Bregengard C, Bjorn SE, Norris K, Gliemann J, and Christensen EI (1995) Evidence that epithelial glycoprotein 330/megalin mediates uptake of polybasic drugs. *J Clin Invest* **96:**1404–1413.
Pan W, Kastin AJ, Zankel TC, van Kerkhof P, Terasaki T, and Bu G (2004) Efficient transfer of receptor-associated protein (RAP) across the blood-brain barrier. *J Cell Sci* **117:**5071–5078.
Pardridge WM (1999) Blood-brain barrier biology and methodology. *J Neurovirol* **5:**556–569.
Pardridge WM (2001) Brain drug targeting and gene technologies. *Jpn J Pharmacol* **87:**97–103.
Pardridge WM (2005) The blood-brain barrier: bottleneck in brain drug development. *NeuroRx* **2:**3–14.
Pardridge WM (2006) Molecular Trojan horses for blood-brain barrier drug delivery. *Curr Opin Pharmacol* **6:**494–500.
Pardridge WM (2007a) Blood-brain barrier delivery. *Drug Discov Today* **12:**54–61.
Pardridge WM (2007b) Blood-brain barrier delivery of protein and non-viral gene therapeutics with molecular Trojan horses. *J Control Release* **122:**345–348.
Peng T, Liu YH, Yang CL, Wan CM, Wang YQ, and Wang ZR (2004) A new peptide with membrane-permeable function derived from human circadian proteins. *Acta Biochim Biophys Sin* **36:**629–636.
Schaadt BK, Hendel HW, Gimsing P, Jonsson V, Pedersen H, and Hesse B (2003) 99mTc-aprotinin scintigraphy in amyloidosis. *J Nucl Med* **44:**177–183.
Shibata M, Yamada S, Kumar SR, Calero M, Bading J, Frangione B, Holtzman DM, Miller CA, Strickland DK, Ghiso J, et al. (2000) Clearance of Alzheimer's amyloid-ss(1–40) peptide from brain by LDL receptor-related protein-1 at the blood-brain barrier. *J Clin Invest* **106:**1489–1499.
Sojan SM, Smyth DR, Tsopelas C, Mudge D, Collins PJ, and Chatterton BE (2005) Pharmacokinetics and normal scintigraphic appearance of 99mTc aprotinin. *Nucl Med Commun* **26:**535–539.
Tsuji A and Tamai II (1999) Carrier-mediated or specialized transport of drugs across the blood-brain barrier. *Adv Drug Deliv Rev* **36:**277–290.
Zhou R, Mazurchuk R, and Straubinger RM (2002) Antivasculature effects of doxorubicin-containing liposomes in an intracranial rat brain tumor model. *Cancer Res* **62:**2561–2566.

Address correspondence to: Dr. Richard Béliveau, Laboratoire de Médecine Moléculaire, Centre d'Hémato-Oncologie, Hôpital Ste-Justine-Université du Québec à Montréal, Montréal, QC, Canada H3C 3P8. E-mail: beliveau.richard@uqam.ca